Ionic liquid ferrofluid electrospray with EMIM-NTf2 and ferrofluid mode studies with FerroTec EFH-1 in a non-uniform magnetic field

IEPC-2013-319

Presented at the 33rd International Electric Propulsion Conference,
The George Washington University • Washington, D.C. • USA
October 6 – 10, 2013

Edmond J. Meyer IV[1] and Lyon B. King[2]
Michigan Technological University, Houghton, MI 49931, USA

Nirmesh Jain[3] and Brian S. Hawkett[4]
University of Sydney, NSW, 2006, Australia

Abstract: An electrospray ion source was operated using a newly designed ionic liquid ferrofluid based on the ionic liquid EMIM-NTf2. The magnetic properties of the fluid were exploited to create self-assembling array of peaks on the fluid surface, which were then amplified using an electric field, eventually causing ions to be emitted from the tip of each peak in the instability. A beam current of 72 micro-Amps was measured from a five-peak array subject to extraction voltage of 2750 V. In a separate experiment, modal patterns in the surface of a ferrofluid subject to a Rosensweig instability were measured in non-uniform fields created by permanent magnets. These measured wavelengths were shown to agree well with a hypothesis put forth by Rupp where the magnetic force is treated similarly to the gravitational force in the classical dispersion relation.

Nomenclature

B	=	Magnetic Flux Density
g	=	Acceleration due to gravity
H	=	Magnetic Field
λ_c	=	Critical Wavelength
λ	=	Wavelength
μ_0	=	Permeability of Free Space
μ_r	=	Relative Permeability
$\mu_{viscosity}$	=	Dynamic Viscosity
v	=	Kinematic Viscosity
q	=	Wave number
ρ	=	Fluid Density
ω	=	Instability Growth Rate
σ	=	Surface Tension

[1] Graduate Research Assistant, Mechanical Engineering, 1018 RL Smith Bldg. 1400 Townsend Dr.
[2] Professor, Mechanical Engineering, 1014 RL Smith Bldg, 1400 Townsend Dr.
[3] Graduate Research Assistant, School of Chemistry and Key Centre for Polymers and Colloids, Chemistry F11
[4] Associate Professor, School of Chemistry and Key Centre for Polymers and Colloids, Chemistry F11

I. Introduction

TRADITIONAL electrospray thrusters use arrays of solid structures to support the propellant, enhance the electric field, and provide a means to stress the fluid into having a curved free surface. These support structures can take the form of arrays of capillaries, solid needles, and porous needles or ridges. Linear arrays have been manufactured from sheets of metal, such as porous tungsten and using wet chemical etching techniques to create the peaks.[1, 2] These linear arrays are then aligned with slits in the extraction electrode and coated in a propellant, such as ionic liquid. Each linear array has good packing density, but the array-to-array spacing is generally larger yielding a lower overall packing density.

Planar arrays of tips have been fabricated using materials such as silicon and porous metals.[3-6] Tens to hundreds of single emitter tips are etched into the base material using wet etching processes coupled with photolithography. Once these emitters are created they are then aligned and assembled with an extraction grid with the same spacing and alignment of holes. Both the solid and porous planar arrays are passively fed propellant by capillary action and by the electric field.

Another common type of planar array uses capillaries instead of a solid or porous substrate. Capillaries are fabricated using wet etching techniques coupled with photolithography in silicon. An example of one such device is a 19 emitter array developed by Krpoun and Shea.[7] The capillaries are then filled with fused silica beads to control the hydraulic impedance. Another type of capillary planar array was developed by Busek, and each individual capillary was micromachined and later assembled into an array of capillary emitters.[8] With the capillary emitters, a mass flow rate is set and actively controlled for the thruster.

The common trait of all the current state-of-the-art electrospray thrusters is that they all have a support structure for the fluid which confines the fluid, helps transport the fluid, increases the local electric field, and stresses the fluid into being "curved". The issue with all of these structures is that they can be easily and permanently damaged either when fabricated, during assembly and transport or while operating. What is required to induce electrospray in a conductive fluid is (1) a strong starting electric field (~10^7 V-m^{-1}), and (2) a fluid surface having a small radius of curvature to create a Taylor cone, which increases the local electric field high enough to extract ions from the cone tip. Conventional liquids do not want to form small-radius features naturally; therefore, a support structure is required to force the fluid to demonstrate a small radius of curvatures.

In 2012 Meyer and King demonstrated electrospray using a new class of fluid that was capable of naturally forming small-radius features with needles or capillaries.[9] This new type of fluid class is called an ionic liquid ferrofluid (ILFF), which is a superparamagnetic, conductive, room temperature ionic liquid with low vapor pressure. ILFFs can be stressed by both electric and magnetic fields. Applying a magnetic field to this these fluids stresses the fluid surface, creating a stable series of self-arranging peaks known as a Rosensweig instability. An applied electric field further stresses and deforms the fluid causing the peaks amplitude to increase and tip radius to decrease. A sufficiently strong electric field was shown to cause electrospray emission from the fluid peaks.

The initial work of Meyer and King demonstrated ionic liquid ferrofluid electrospray using the hydrophilic ionic liquid Ethylammonium Nitrate (EAN) doped with Sirtex magnetic nanoparticles.[9] Work reported here extends this early progress by duplicating the test using a hydrophobic ionic liquid that would be more suitable for space propulsion. Additionally, this paper reports on early efforts towards understanding scaling issues for an ionic liquid ferrofluid electrospray array. Specifically, studies are conducted on a conventional ferrofluid (not based on ionic liquid) to understand the relationship between the strength and gradient of an applied magnetic field and the tip-to-tip emitter "packing density" displayed by the ferrofluid.

This paper begins with a background on ferrofluid dynamics, known as ferrohydrodynamics, and presents the theory for spatial mode shapes for Rosensweig instabilities in a pool of ferrofluid under uniform magnetic field. Following this the authors examine a proposed change to the existing theory that can account for non-uniform magnetic fields. This will be followed by a description of the ionic liquid ferrofluids used in this study. After that, the goal of the work will be presented, followed by a description of the experimental setup for both of the experiments conducted and presented in this work. The results for both sets of experiments will then be presented, and the paper will then finish with a conclusion on the work.

II. Background

A. Ferrofluids

Ferrofluids are unique liquids that do not occur in nature, but have existed since their first laboratory creation in the 1960's. Ferrofluids differ from magnetorheological fluids (MR fluids) by the size of the suspended particles: ferrofluids have particles on the order of 10nm, while particles in MR fluids can be many microns. An excellent description of ferrofluid dynamics can be found in the books by Rosensweig[10] and Odenbach.[11] Ferrofluids are formed when nanometer-sized ferromagnetic particles are permanently suspended within a carrier liquid. The particles are small enough that Brownian motion keeps them from settling out of the liquid due to gravity or magnetic forces. The particles are also small enough (~10nm) so that they possess a single magnetic domain, thus the resulting colloidal fluid is superparamagnetic. The magnetic particles are often coated with a surfactant to prevent agglomeration and sedimentation, although this isn't always necessary. Common carrier liquids are mineral oils, kerosene, and water. The focus of this paper is ferrofluid created using ionic liquid as the carrier; these fluids are described in Section III.

The motion and behavior of a ferrofluid is described by the field of ferrohydrodynamics, which couples the Navier-Stokes equations with the Maxwell magnetostatic relations. The fluids have rich and complex non-linear motion, since they both respond to applied magnetic fields while also altering the magnetic field because of their superparamagnetic behavior. The most well known and dramatic response of a ferrofluid is the so-called Rosensweig instability,[12, 13] which is the subject of this paper. The Rosensweig instability results when a perturbation in the surface of the ferrofluid causes a bunching of the magnetic field lines as depicted in the left most image of Figure 1. The bunching of the field lines, which represents a spatial gradient in the field strength, attracts ferrofluid to the strong-field region at the tips of the perturbation. As a result, the height of the fluid perturbation will increase and the field lines will be more dramatically pinched such that the field at the tip will be increased even more, attracting more fluid to the tip ad infinitum. The instability is arrested by fluid surface tension, which seeks to minimize free surface area. When a pool of ferrofluid is subject to a moderate external magnetic field the resulting surface instability can be thought of (with extreme care) as the magnetic analog of the electrostatic Taylor cone. An image of a static Rosensweig instability is shown in the rightmost image of Figure 1. From an energy standpoint the Rosensweig instability represents a balance between the magnetic interaction energy of the fluid which is reduced by the peak geometry, and the surface tension energy, which is increased by the non-planar surface. The peaks themselves can display complicated geometry as shown Figure 2, where a secondary magnetic instability is seen on the apex of each primary tip. Depending upon the depth of the fluid pool Rosensweig instabilities can create discrete peaks having no fluid between them, as in Figure 2, or as a singular continuous fluid with spikes on the surface as in Figure 1.

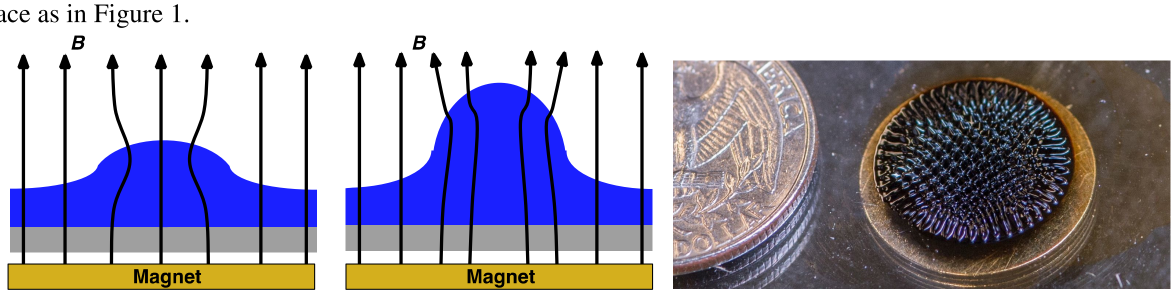

Figure 1: Left: a perturbation in the surface of the ferrofluid causes a local bunching of magnetic field lines. Center: ferrofluid is attracted to the strong-field region, amplifying the perturbation and further increasing field gradient. Right: A puddle of ferrofluid is shown on a small permanent magnet (note U.S. quarter in image). The static pattern of sharp fluid spikes in the liquid surface is known as a Rosensweig instability.

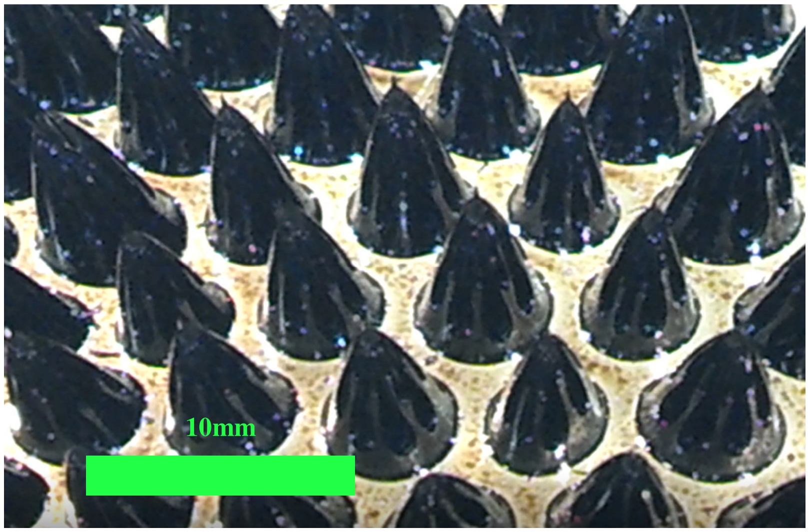

Figure 2: Close-up image of Rosensweig instability in a ferrofluid showing discrete peaks separated by regions of no fluid. Also note secondary instability peaks forming on the apex of each primary peak.

The classical derivation of Rosensweig instability modes assumes that gravity acts parallel to a uniform applied magnetic field such as that generated in the bore of a Helmholtz configuration of electromagnets. A dispersion relation describing the spatial wavelength of peaks then is derived by balancing gravitational, magnetic, and surface tension energy with the results shown in Equation (1).[14] The dispersion relation assumes that a uniform magnetic field is applied normal to the unperturbed surface of a fluid pool with infinite depth (equal to or thicker than the capillary length) and infinite lateral dimension.[15] The fluid parameters expressed in Equation (1) are ν - the kinematic viscosity, ρ - the fluid density, σ - surface tension, and μ_r, the relative permeability of the fluid. Constants in Equation (1) are g - the acceleration due to gravity, and μ_0 - permeability of vacuum. The variables in Equation (1) are ω - the growth rate of the peaks, q - the wave number, and B - the applied magnetic field. At onset of instability, meaning when the magnetic field strength is barely sufficient to induce an instability, $\omega = 0$ and the dispersion relation describes a stationary mode where the wavelength is the capillary length, Equation (3). The wave number, q, and the wavelength, λ, are related through Equation (2). As the magnetic field strength increases beyond the minimum value for onset the dispersion relation predicts that the peak spacing will increase in magnitude beyond the capillary length.[15]

$$\left(1-\frac{i\omega}{2\nu}\right)^2+\frac{1}{4\rho\nu^2q^4}\left[\rho g q+\sigma q^3-\frac{(\mu_r-1)^2}{(\mu_r+1)\mu_0\mu_r}B^2q^2\right]=\sqrt{1-\frac{i\omega}{\nu q^2}} \quad \textbf{(1)}$$

$$\lambda=\frac{2\pi}{q} \quad \textbf{(2)}$$

$$\lambda_c=2\pi\sqrt{\frac{\sigma}{\rho g}} \quad \textbf{(3)}$$

Lange et al. performed an experiment measuring the spacing of the observed hexagonal pattern in a ferrofluid Rosensweig instability and found results that seemed to disagree with theory: the peak spacing was observed to be very close to the capillary wave number (~650 m^{-1} measured vs. 614 m^{-1} predicted), however the spacing was invariant with respect to the applied magnetic field.[16] Later experiments by Gollwitzer et al, were able to measure an increase in wavelength of the peaks with an increase in applied magnetic field as predicted by theory, with the wavelength at onset approximately the capillary length of the fluid, all as predicted by the dispersion relation.[17] The difference in the two experiments was the boundary conditions. In the work by Lange et al., the pool boundary consisted of vertical edges, while in the work by Gollwitzer et al., the boundary was a "beach" where the edges of fluid container were sloped up at 32°, allowing a looser boundary. The fixed wavelength observed in the work by Lange et al. was likely influenced by the boundary conditions of the container, which permitted only discrete numbers of peaks between the edges thus preventing the gradual increase in peak spacing described by theory.

Rosensweig instabilities are easily excited by permanent magnets, however the resulting features demonstrate some differences when compared to the instability described by Equation (1). Unlike the uniform field assumption in the classical derivation, finite-sized permanent magnets possess inherent field gradients. Rosensweig instabilities in non-uniform fields show two behaviors that depart from classical theory: (1) The gradient in the magnetic field exerts a body force attracting the bulk ferrofluid to the magnet and this force can be much stronger than gravity, and (2) The peak spacing observed on fluid surfaces excited by permanent magnets can be much smaller than peaks generated by an equivalent-strength uniform magnetic field. One such example of this is the rightmost image of Figure 1: the capillary length of the fluid shown in this image is approximately 10 mm, however 14 peaks can be observed within a 25 mm length (roughly 1.8 mm wavelength). From this observation, it would appear that the gradient of the magnetic field plays an important role in the wavelengths. Furthermore, the effect of gravity on the instability shown in Figure 1 is negligible - a fact that can be proven by orienting the magnet and fluid in any orientation, including upside-down, and noting that the mode shape is unaffected.

The assumptions that were critical in deriving Equation (1) are clearly not relevant for a ferrofluid instability excited by a permanent magnet. Surprisingly, a compatible theory could not be located in literature. The only treatment of non-uniform fields in literature is a brief and untested hypothesis put forward by Rupp. In Rupp's dissertation, Rupp and Shliomis proposed that the strong magnetic body force exerted on the fluid by a permanent magnet can replace the gravity term used in the classical derivation.[18] They justified this by comparing the volumetric body force due to the magnetic field gradient to that of gravity, as shown in Equation (4). In Rupp's work, they found that the body force of the magnetic gradient can easily be an order of magnitude stronger than that of gravity (a statement that is supported by the ability to invert a ferrofluid-on-magnet arrangement with no change in structure). The hypothesis they put forward was to simply replace ρg with the magnetic body force, which scales with $B\nabla B$, in the classical derivation, resulting in an expression for the instability peak wavelength given in Equation (5). This predicts that if the fluid body forces are dominated by the magnetic gradient instead of gravity, the wavelength should decrease with an increase of the product of the magnetic field and its gradient. This prediction appears to have a similar trend as to what has been observed in the rightmost image of Figure 1, but no literature has been found testing this prediction.

$$\frac{f_{gradient}}{f_{gravity}} = \frac{B\nabla B}{\mu_0 \mu_r \rho g} \tag{4}$$

$$\lambda = 2\pi \sqrt{\frac{\mu_0 \mu_r \sigma}{B\nabla B}} \tag{5}$$

B. Ionic Liquid Ferrofluids

In 2011 Jain and Hawkett[19] successfully synthesized the first ferrofluid based on an ionic liquid carrier shortly followed by Huang and Wang in 2012[20] (note that other groups including Oliveira in 2009[21] and Rodriquez-Arco in 2011[22] have also pursued ionic liquid ferrofluids, but were unable to create stable suspensions that demonstrated the hallmark Rosensweig instability). The resulting ionic liquid ferrofluid still obeys classical ferrohydrodynamics and displays the Rosensweig instability, however unlike past water- and oil-based ferrofluids the ILFF is also highly conductive with almost zero vapor pressure.

Jain et al were able to create a number of stable ILFFs.[19] The first two ILFFs they were able to create using bare maghemite nanoparticles (Fe_2O_3 with no surfactants) with EMIM-Ac (1-ethyl-3-methylimidazolium acetate) and EMIM-SCN (1-ethyl-3-methylimidazolium thyocyanate). By adding a surfactant of acrylic acid-b-acrylamide copolymer to the magnetic nanoparticles, they were able to create a stable ILFF in EAN (Ethylammonium nitrate). All three of the ILFFs described were stable for at least months (they are still stable at the time of this writing) and exhibited the Rosensweig instability when a magnetic field was applied.

In early 2013, a hydrophilic ILFF was created by Jain and Hawkett group again using EAN, but this time with proprietary magnetic nanoparticles provided by Sirtex. This ILFF was used in the first-ever proof-of-concept demonstration of an electrospray ion source utilizing an ILFF and the Rosensweig instability.[9] At room temperature, this early fluid prepared using EAN with Sirtex magnetic nanoparticles had a high viscosity, and thus instability peaks formed in "slow motion," taking some tens of seconds to react to changes in electric and magnetic fields. The ammonium based IL was also protic, and absorbed water out of the ambient air. Recently a new hydrophobic ILFF has been designed and created by Jain and Hawkett, 1-Ethyl-3-methylimidazolium bis(trifluoromethylsulfonyl)imide (EMIM-NTf2) with Sirtex magnetic nanoparticles. This fluid was developed with the goal of creating a more water-tolerant ILFF for in-vacuum use as well as reducing the ILFF viscosity below that of the EAN-based sample. Unlike the EAN-based fluid with Sirtex magnetic nanoparticles, the EMIM-NTf2 with Sirtex magnetic nanoparticles has a viscosity similar to water. The thermal stability of the new EMIM-NTf2 based ILFF is ~350°C compared to ~200°C for the EAN based ILFF. The EMIM-NTf2 ILFF is aprotic, and does not have the propensity to absorb water from the ambient air.

III. Goal of Work

This work reports on two separate experiments with different goals. The purpose of the first experiment, which we will refer to as Experiment 1, was to expand on prior work and explore an ILFF-based electrospray source with an improved fluid. In the original work, EAN with Sirtex magnetic nanoparticles was not designed with ion emission in a vacuum in mind, but for a biomedical purpose and so this fluid was not ideal for in-vacuum application. The goal of the present work was to test a new ILFF (EMIM-NTf2 with Sirtex magnetic nanoparticles) specifically designed to be used for electrospray in vacuum and to compare its performance against the EAN-based liquid.

The second experiment discussed in this work, which we will refer to as Experiment 2, was designed to test Rupp's hypothesis concerning the peak spacing of Rosensweig instabilities excited by the non-uniform fields of permanent magnets. For this work a traditional commercially available oil-based ferrofluid was used (no electrospray). Surface instabilities excited by permanent magnets were imaged and the observed peak spacing was compared to the hypothesis put forth by Rupp. The motivation for this test was to understand how peak spacing depends on magnetic field shape.

IV. Experiment Design

A. Experiment 1 Design: ILFF electrospray apparatus

The purpose of the electrospray apparatus was to contain the ILFF, apply magnetic and electric fields to the fluid, measure the current of emitted ions, and provide optical imaging access during the testing. The ILFF utilized for this experiment was a new fluid not previously reported in literature. The ILFF was created by sterically stabilizing maghemite nanoparticles synthesized by Sirtex in the ionic liquid EMIM-NTf2, which is hydrophobic.

An illustration of the cross section of the test apparatus can be viewed in Figure 3. The ILFF was placed in a 2-mm-wide, 2-mm-deep, 8-mm-diameter trench in an aluminum block that provided electrical contact to the fluid, as shown in the middle image in Figure 4. The extraction electrode was placed 4.6 mm above the aluminum fluid holder, meaning the gap between the ILFF and the extraction electrode was smaller than 4.6 mm since the fluid peaks grow above the rim of the trench. The extraction electrode, shown in the right of Figure 4, had an annular pattern (broken by three support spokes) that permitted extracted ions to pass to a downstream current collector, which was made from ITO glass. A stack of 5 grade-N52 3.2-mm-thick, 25.4-mm-diameter magnets were placed below the ILFF causing 5 peaks to form in the fluid, as shown in Figure 5.

The extraction voltage was provided by a Glassman FX +25 kV power supply. The extraction electrode was grounded, and the fluid was biased positively. Current was measured at the ITO glass collector using a Keithly 2410 sourcemeter, referenced to ground (extraction grid). For all testing, a single polarity was used.

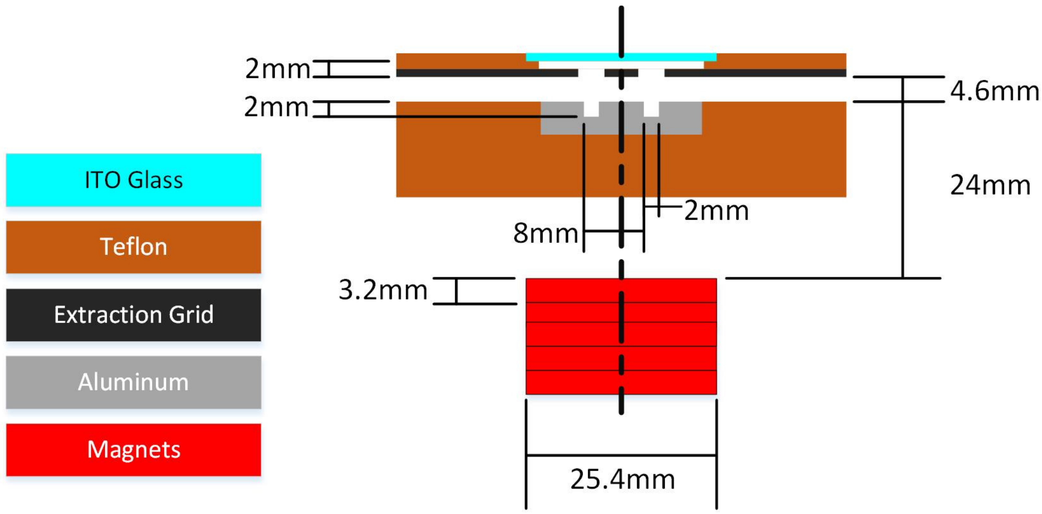

Figure 3: Illustration of cross-section of Experiment 1

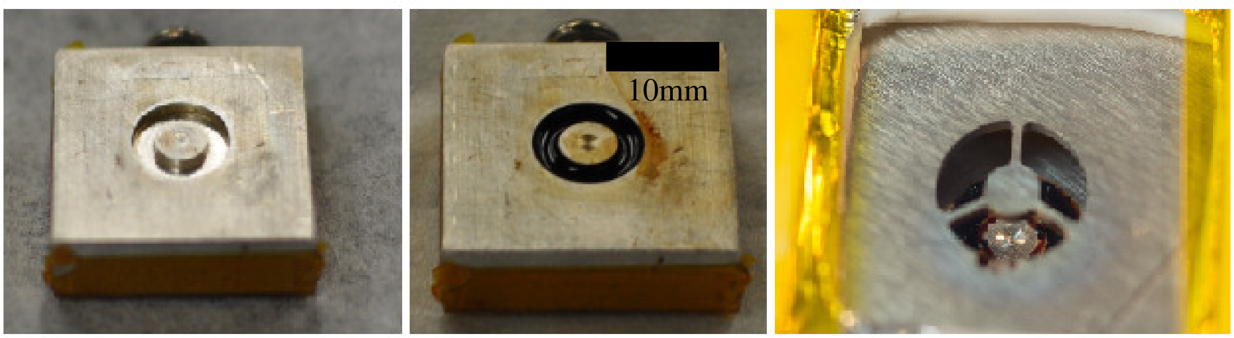

Figure 4: Left: Fluid Holder. Middle: Fluid Holder with ILFF. Right: Fluid Holder with ILFF with extraction electrode and current collector placed above.

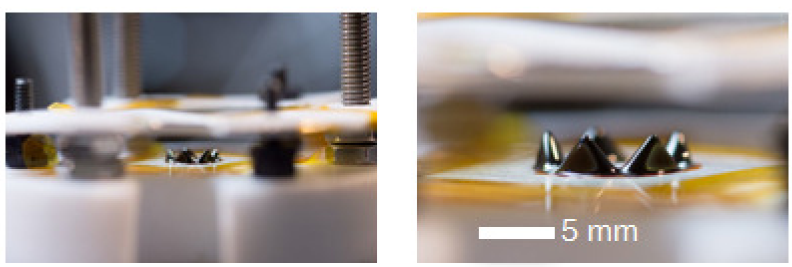

Figure 5: Experimental Setup. Left: Side view of the extraction electrode and tips. Right: Close up image of the tips.

B. Experiment 2 Design: Wavelength measurement in a non-uniform magnetic field

The purpose of this experimental setup was vary the value of $B\nabla B$, measure the wavelengths of the instabilities, and then compare the measured instability wavelengths to wavelengths predicted by Rupp in Equation (5). The method of varying $B\nabla B$ was to use multiple magnets and multiple spacings between the fluid pool and the magnets. Because the magnets are of finite size, the field lines are non-uniform, as shown in Figure 6. The strength of the magnetic field weakens, as does the gradient of the magnetic field, as one moves farther away from the magnet surface, so in principle the value of $B\nabla B$ can be varied by manipulating the distance between the liquid pool and the magnet surface. However, the intrinsic variation of $B\nabla B$ in the lateral (radial) direction poses an experiment design problem.

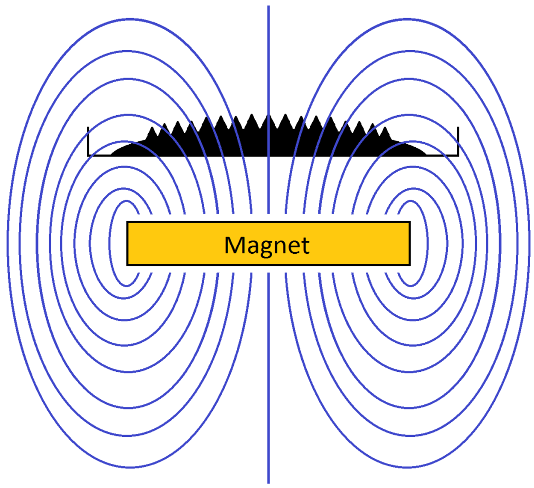

Figure 6: Illustration of magnet with magnetic field lines drawn, and instabilities in a ferrofluid

It is not possible to create a magnetic field where the value of B∇B is constant in magnitude or direction throughout the entire volume of a liquid pool. For instance, in the configuration shown in Figure 6 the value of B∇B varies both laterally (radially) across the pool surface as well as vertically within the shallow pool. Thus, it is not clear which value of B∇B to use when evaluating Rupp's hypothesis. For this work, the authors chose to use the value of B∇B along the centerline of the magnet at the surface of the liquid pool to provide some comparison with the prediction of Rupp. The consequences of this convention will be discussed in the Results section. In order to compare the measured instability wavelengths to the values predicted by Equation (5), the centerline axial magnetic field was measured along magnet centerline every 0.5 mm for each magnet, starting at the magnet surface using an Alpha Labs GM-2 Gaussmeter.. The gradient was calculated by numerically differentiating the measured magnetic field magnitude profile, thus the effect of radial gradient was ignored. The B∇B was found by multiplying the magnetic field and magnetic field gradient at every location.

The fluid used for Experiment 2 was a commercially available ferrofluid, EFH-1 produced by FerroTec. The stated properties of EFH-1 are listed in Table 1. Roughly 1.6 mL of EFH-1 was placed in a 100-mm-diameter glass Petri dish. Various magnets were placed below the Petri dish and a micro-positioning stage was used to change the gap between the Petri dish and the magnet, effectively changing the value of B∇B at the surface of the pool. The magnet-to-Petri-dish spacing was adjusted in 0.5-mm or 1.0-mm increments using the micro-positioning stage. In order to calculate a theoretical wavelength for each Petri dish location the magnitude of the B∇B field was taken to be the pre-measured value that correlated with the location of the top of the fluid pool (base of the instability peaks), as denoted in Figure 7. This required the thickness of the ferrofluid pool to be known at each measurement location. The thickness was measured at every magnet-to-Petri-dish spacing because it was observed that a ferrofluid pool of constant volume would increase in diameter and decrease in thickness as the ferrofluid pool was farther from the magnet (lower magnetic gradient body forces). It was noted in initial testing that when the magnet-to-Petri-dish spacing was held constant, but the volume of ferrofluid in the dish was varied, thus changing the fluid thickness, drastically different peak spacings were observed including cases where no peaks would form for sufficiently deep pools. The case where no peaks were observed with a very thick fluid directly above the magnet corresponded to roughly the same spacing (magnet-to-Petri-dish plus fluid thickness) of a much thinner fluid that failed to yield Rosensweig instabilities. This implied that the location of the B∇B field that influences the Rosensweig instability formation and instability wavelength was located at the top of the fluid pool (base of the instabilities).

Table 1: FerroTec EFH-1 Fluid Properties

Surface Tension, σ	Density, ρ	Viscosity, $\mu_{viscosity}$	Relative Permeability, μ_r	Capillary Length, λ_c
29mN-m^{-1}	1210 kg-m^{-3}	6 mPa-s	2.6	9.82 mm

A Nikon D5000 camera and an AF-S Micro Nikkor 60-mm f/2.8G ED lens were used to image the peaks formed in the ferrofluid. After capturing an image of the ferrofluid, the pool of ferrofluid would be replaced by a reference grid of known dimensions and a second image would be captured so that the pixels could be correlated to spatial distances during processing. The setup of the system can be viewed below in Figure 7.

Peak spacing was measured only for the few peaks that comprised the center "unit cell" of each instability modal pattern. This was because the center peaks should (1) have the least influence from any radial magnetic field component, and (2) the peaks in the center should have smallest influence from the boundary of the fluid, and (3) the value of $B\nabla B$ at the center of the fluid pool was used for comparison with Rupp. After the pixel location of the center peak was chosen, the nearest surrounding peaks were then selected, whether it was 4 peaks for a square pattern (Leftmost image of Figure 8), or 6 for a hexagonal pattern (Rightmost image of Figure 8); other lattice structures have been observed as well, such as 2 or 7. The distances between the center peak and the surrounding peaks were then calculated, and averaged. This value was reported below in Section V Subsection B as the peak spacing. The standard deviation of these values was used as the error in the plots.

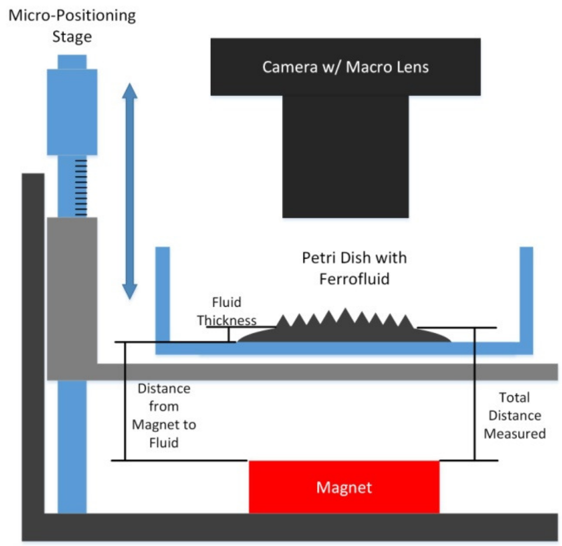

Figure 7: Illustration of Experiment 2

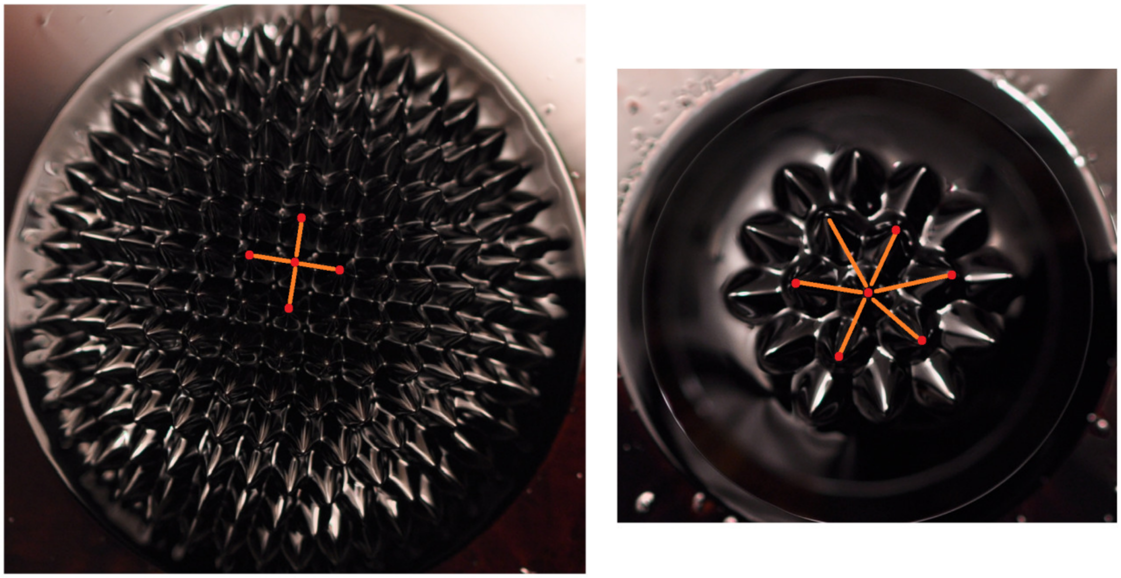

Figure 8: Examples of Instability Patterns. Left: Square Pattern of instabilities, ferrofluid 10.19 mm above 1" diameter by 1/4" magnet λ =2.42 mm. Right: Hexagonal Pattern of instabilities, ferrofluid 11.79 mm above 1/2" diameter by 1/8" magnet λ = 3.83 mm. Note that the pure hexagon cell is distorted due to boundary effects.

V. Results

A. Experiment 1: Electrospray of EMIM-NTf2

Filling the test apparatus described in Section IV Subsection A with EMIM-NTf2 with Sirtex MNPs and then placing a magnet below the test fixture caused the 5 peaks in the left of Figure 9 to form. Applying a voltage between the aluminum block holding the fluid pool and the extraction electrode stressed the ILFF causing the peaks to grow in height and decrease their radius of curvature at the tip. Onset of ion emission was found between 2400 and 2500 V applied between the fluid and the extraction electrode. The applied voltage was increased to 2750 V, resulting in the peaks in the rightmost image of Figure 9, where the ion current measured from the array was approximately 72 µA.

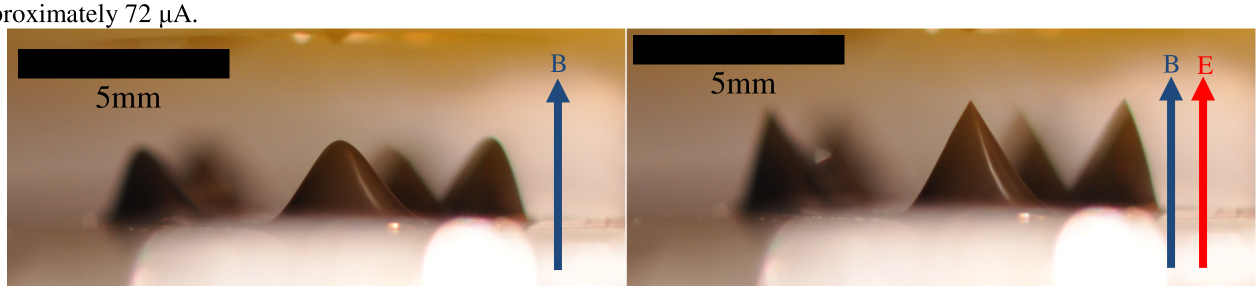

Figure 9: EMIM-NTf2 in test setup with the extraction electrode at the top of the images and the magnetic and electric fields applied vertically. Left: No applied voltage. Right: 2750 V applied, emitting ions.

The trace in Figure 10 shows a typical current-voltage characteristic of the spray emission. Current and voltage telemetry were measured and recorded every 0.5 seconds. While data are somewhat limited, it is still instructive to compare emission characteristics of the EMIM-NTf2 ILFF with that of the EAN ILFF reported previously.[9] The EMIM-NTf2 based ILFF had a lower onset voltage of 2500 V compared to 3250 V for EAN for the same electrode-to-tip spacing. The array of tips made of EMIM-NTf2 ILFF also yielded a higher peak emission current of 72 µA versus 14 µA for the array with EAN. The EMIM-NTf2 also did not appear to produce any bubbles that temporarily interrupted emission as in the previous testing with EAN.

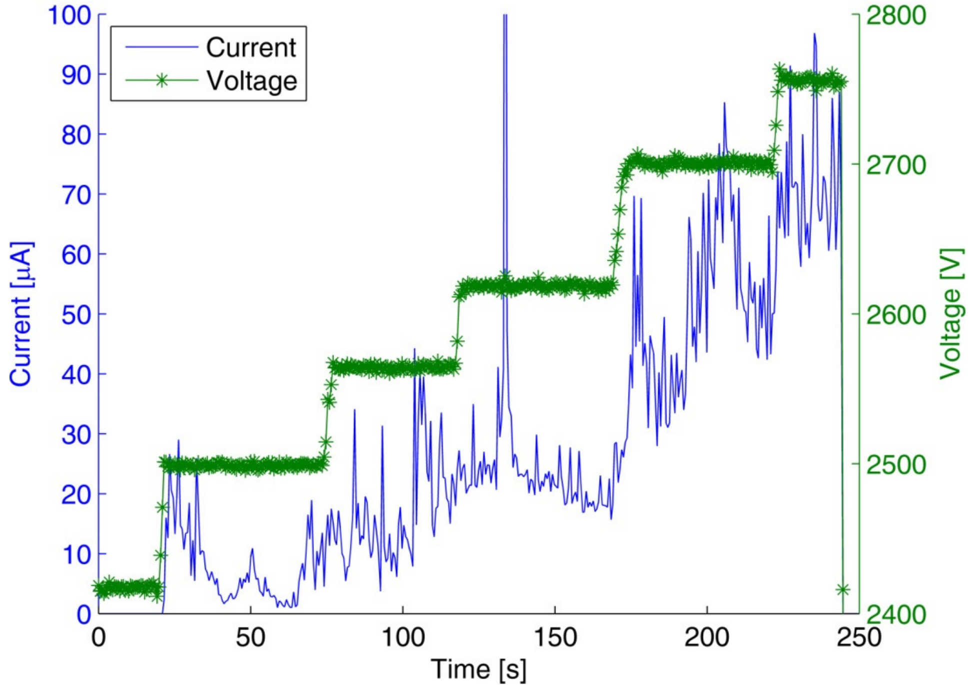

Figure 10: Current and voltage measured over time from a 5-tip array of EMIM-NTf2 with Sirtex MNPs

A behavior that has been observed in both the EAN- and EMIM-NTf2-based ILFFs is spontaneous and unexpected splitting of the tip of the instability into multiple tips. An example of this is shown in Figure 11, were each of the tips of the EMIM-NTf2 array bifurcated into two smaller emission sites. In previous work, up to three emitters were observed with EAN-based ILFF. The cause of the change to multiple emission sites is currently unknown.

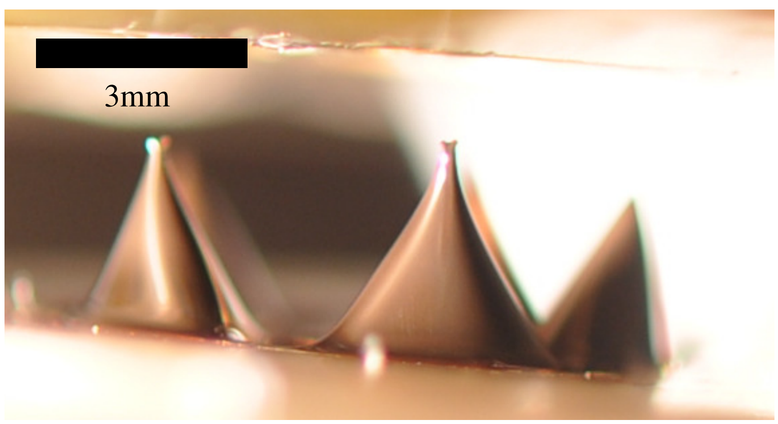

Figure 11: ILFF showing two emission sites from a single peak

B. Experiment 2: Instability Wavelength in Non-Uniform Field

It has been observed that the dispersion relation in Equation (1) does not correctly predict the instability wavelength in a non-uniform magnetic field, which is not un-expected since field uniformity was a key assumption in the derivation. An experiment was conducted to determine if the same dispersion relation could be used albeit with a simple replacement of the gravity body force, ρg, with the magnetic gradient body force, which scales with B∇B. In order to accomplish this, instability wavelengths were measured in various B∇B fields and compared to the predicted wavelengths by Equation (5).

The ferrofluid used for Experiment 2 was EFH-1 manufactured by FerroTec. The properties of this fluid were given previously Table 1. The instability wavelengths predicted by Equation (5) versus B∇B is shown as the solid black trace in **Figure 12**. The instability wavelengths of the ferrofluid above various magnets are shown in **Figure 12** as the dashed lines with the error bars, where the value of B∇B was taken on magnet centerline at the surface of the fluid pool for each data point. All of the data follow the same trend as predicted by Equation (5), namely that peak spacing seems to scale with $\sqrt{B\nabla B}^{-1}$. The data set in cyan, reporting the instability wavelengths of the 1" diameter by 1/4" thick magnet, has the best agreement in the region of B∇B = 0.38 T^2-m^{-1} and higher with Rupp's hypothesis, while the green trace indicating the instability wavelengths of the 3/4" diameter by 1/8" thick magnet data set had the best agreement in the range of 0.062 < B∇B < 0.28 T^2-m^{-1}. The data sets corresponding to the instability wavelengths measured using the 1/2" by 1/8" magnet, 3/4" by 1/8" magnet and 1" by 3/8" magnet are very comparable to the predicted instability wavelength. The left portion of the trace corresponding to B∇B < 0.06 T^2-m^{-1} the instability wavelengths measured on a 3/4" diameter by 1/8" thick magnet appears to be "flat" or the instability wavelength does not change with B∇B. Such strange behavior at low values of B∇B are likely due to finite-pool boundary effects. The dispersion relation of Equation (1) is based on an infinite fluid. For large values of B∇B there are many peaks across the surface of the pool, such that the center-most peaks are somewhat isolated from the peripheral boundary conditions. In these instances the center region of the pool will demonstrate behavior consistent with an infinite reservoir. However, at low values of B∇B the peak spacing becomes so large that only a few peaks span the entire fluid surface. In these instances the peripheral boundary conditions certainly have a strong role in determining peak spacing and infinite-pool behavior is not expected.

While the predictions of Rupp’s hypothesis show fairly good agreement with observation, the inability to make an exact comparison exposes a shortcoming in the approach. The classical dispersion relation derived as Equation (1) makes two key assumptions: (1) the fluid pool is infinite in depth and lateral dimension, and (2) the gravity body force and the magnetic field are uniform (no spatial gradients) throughout the pool. While the simple approximation of Equation (5) is derived from the logical reasoning that any strong body force acting normal to the fluid surface can act as the “gravity” term in Equation (1), it is strictly in conflict with the assumptions used to derive Equation (1). Specifically, the gradient of any real non-uniform magnetic field varies spatially such that it is not possible to have a uniform value of B∇B throughout the volume of a fluid pool. The value of B∇B will vary both along the surface of the pool as well as throughout the pool depth. Thus it is not possible to define “the” value of B∇B for a given pool of ferrofluid. Furthermore, the surface instability pattern described by Equation (1) is not a point property where the local peak spacing can be related to the local value of the field properties, but instead is a global behavior that arises from energy minimization. These key differences in field behaviors make it impossible to precisely compare Rupp’s hypothesis with a real instability created by a non-uniform field. Nevertheless, the trend predicted by Rupp is convincingly similar to that observed from experiment.

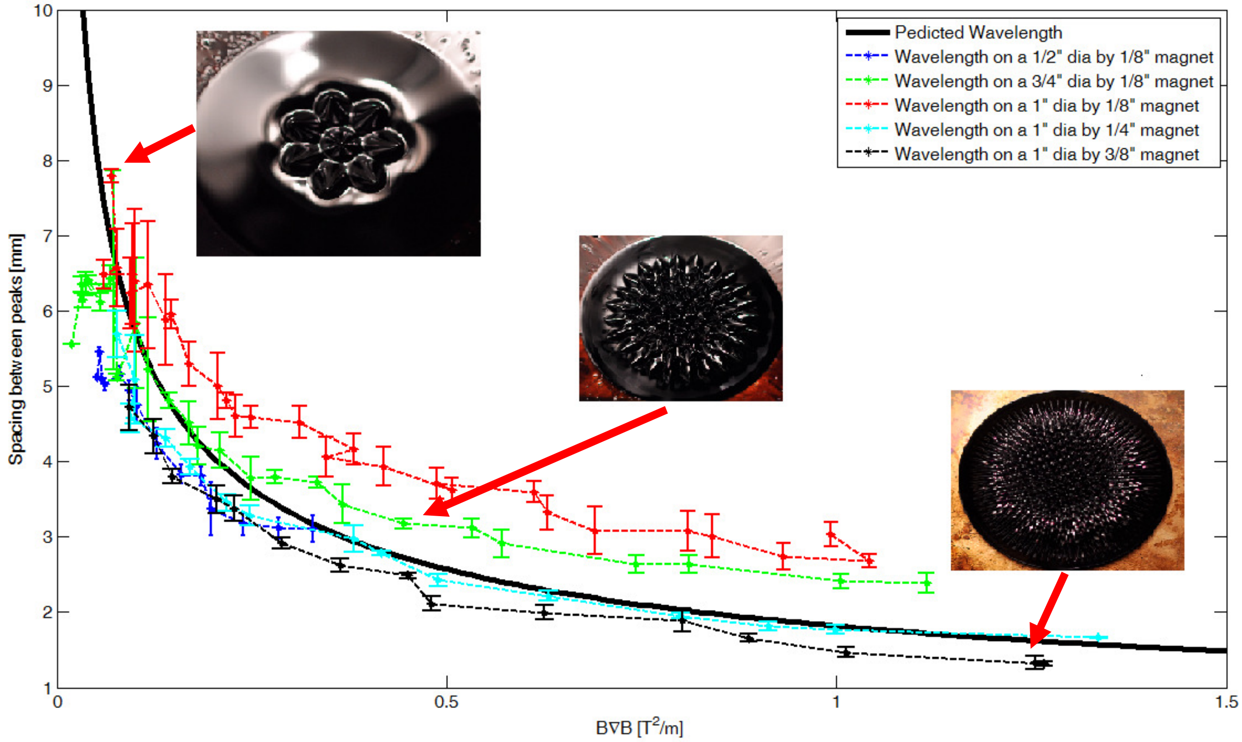

Figure 12: Measured vs. Predicted wavelengths of EFH-1 in various B∇B fields

VI. Conclusion

An electrospray ion source was operated using a newly designed ILFF, EMIM-NTf2 with Sirtex magnetic nanoparticles. The peak emission current from the array was 72 μA, or five times higher than previously measured in the same experimental setup using a ferrofluid based on EAN with Sirtex magnetic nanoparticles. the EMIM-NTf2 also had a lower ion emission onset voltage of approximately 2500 V compared to 3250 V for the EAN-based ILFF. Multiple emission sites on a single peak were observed in the EMIM-NTf2-based ILFF in this work similar to what was noted in prior tests with EAN-based ILFF.

Instability wavelengths of a ferrofluid in a non-uniform magnetic field were studied for the first time. The overall trend of peak spacing as a function of B∇B was found to agree well with the wavelength predicted by Rupp. However, the study exposed a limitation in Rupp's hypothesis, namely that it is not possible to create a non-uniform field where the value of B∇B is a constant throughout a volume of ferrofluid. Despite this, when the value of B∇B was taken to occur on magnet centerline at the pool surface the observed spacing agreed reasonably well with Rupp's model.

Acknowledgments

This work was funded by the AFSOR as a part of the Michigan/Air Force Center of Excellence in Electric Propulsion under contract FA9550-09-1-0695.

References

1.Legge, R.S. and Lozano, P., *Maximizing One-Dimensional Porous Emitter Packing Density for Electrospray Applications.*
2.Legge, R.S., Lozano, P. and Martinez-Sanchez, M., *Fabrication and Characterization of Porous Metal Emitters for Electrospray Thrusters*, in *30th International Electric Propulsion Conference, Florence, Italy, September 2007, IEPC-2007-145.*
3.Gassend, B., et al., *A Microfabricated Planar Electrospray Array Ionic Liquid Ion Source With Integrated Extractor.* Journal of Microelectromechanical Systems, 2009. **18**(3): p. 679-693.
4.Courtney, D.G., Li, H.Q. and Lozano, P., *Emission measurements from planar arrays of porous ionic liquid ion sources.* Journal of Physics D: Applied Physics, 2012. **45**.
5.Li, H.Q., et al., *Fabrication and Testing of an Ionic Electrospray Propulsion System with a Porous Metal Tip Array*, in *Solid-State Sensors, Actuators and Microsystems Conference (TRANSDUCERS), Beijing, China, June 2001.*

6.Lozano, P. and Courtney, D.G., *On the Development of High Specific Impulse Electric Propulsion Thrusters for Small Satellies*, in *Pestana conference Center - Funchal, Madeira - Portugal, May-June 2010*.
7.Krpoun, R. and Shea, H.R., *Microfabricated out-of-plane arrays of integrated capillary nano-electrospray emitters*, in *31st International Electric Propulsion Conferene, Ann Arbor, MI, September 2009, IEPC-2009-188*.
8.Spence, D., Demmons, N. and Roy, T., *A Compact Low-Power High-Isp Thruster for Microsatellites*, in *22nd Annual AIAA/USU Conference on Small Satellites, August 2008, SSC08-VII-4*.
9.Meyer, E.J. and King, L.B., *Electrospray from an Ionic Liquid Ferrofluid utilizing the Rosensweig Instability*, in *49th AIAA/ASME/SAE/ASEE Joint Propulsion Conferene & Exhibit, Paper No. AIAA-2013-3823, 14-17 July 2013, San Jose, CA.*
10.Rosensweig, R.E., *Ferrohydrodynamics*: Cambridge University Press 1985.
11.Odenbach, S., *Colloidal Magnetic Fluids: Basics, Development and Application of Ferrofluids*. Lecture Notes in Physics: Springer, 2009.
12.Rosensweig, R.E., *Magnetic Fluids.* Ann. Rev. Fluid Mech., 1987. **19**: p. 437-463.
13.Boudouvis, A.G., et al., *Normal Field Instability and Patterns in pools of ferrofluid.* Journal of Magnetism and Magnetic Materials, 1987. **65**: p. 307-310.
14.Lange, A., *Scaling behaviour of the maximal growth rate in Rosensweig instability.* Europhysics Letters, 2001. **55**(3): p. 327-333.
15.Friedrichs, R. and Engel, A., *Pattern and wave number selectrion in magnetic fluids.* Physical review E, 2001. **64**(2): p. 1-10.
16.Lange, A., Reimann, B. and Richter, R., *Wave number of maximal growth in viscous ferrofluids.* Magnetohydrodynamics, 2001. **37**(3): p. 261-267.
17.Gollwitzer, C., Rehberg, I. and Richter, R., *Via hexagons to squares in ferrofluis: experimments on hysteretic surface transformations under variation of the normal magnetic field.* Journal of Physics: Condensed Matter, 2006. **18**: p. S2643-S2656.
18.Rupp, P., *Spatio-teporal Phenomena in a Ring of Ferrofluid Spikes*, 2003, University of Bayreuth.
19.Jain, N., et al., *Stable and Water-Tolerant Ionic Liquid Ferrofluid.* Applied Materials and Interfaces, 2011(3): p. 662-667.
20.Huang, W. and Wang, X., *Study on the properties and stability of ionic liquid-based ferrofluids.* Collloid Polym Sci, 2012. **290**: p. 1695-1702.
21.Oliveira, F.C.C., et al., *Magnetic Fluids Based on gamma-Fe2O3 and CoFe2O4 Nanoparticles Dispersed in Ionic Liquids.* J. Phys. Chem. C, 2009. **113**: p. 8566-8572.
22.Rodriquez-Arco, L., et al., *Stability and magnetorheological behaviour of magnetic fluids based on ionic liquids.* Journal of Physics: Condensed Matter, 2011. **23**: p. 1-15.